AAPS PharmSciTech, Vol. 15, No. 5, October 2014 (© 2014)
DOI: 10.1208/s12249-014-0157-0

Research Article

A 5,7-Dimethoxyflavone/Hydroxypropyl-β-Cyclodextrin Inclusion Complex with Anti-Butyrylcholinesterase Activity

Supachai Songngam,[1] Mongkol Sukwattanasinitt,[2] Krisana Siralertmukul,[3] and Pattara Sawasdee[2,4]

Received 30 January 2014; accepted 20 May 2014; published online 31 May 2014

Abstract. This study aimed to improve the water solubility of 5,7-dimethoxyflavone (5,7-DMF) isolated from *Kaempferia parviflora* by complexation with 2-hydroxypropyl-β-cyclodextrin (HPβ-CD). The phase solubility profile of 5,7-DMF in the presence of HPβ-CD was classified as A_L-type and indicated a 1:1 mole ratio. Differential scanning colorimetry, X-ray diffraction, NMR and SEM analyses supported the formation of a 5,7-DMF/HPβ-CD inclusion complex involving the A ring of 5,7-DMF inside the HPβ-CD cavity. This is the first example of CD inclusion with the A ring of non-hydroxyl flavones. The stability and binding constants of the complexes were determined using the phase solubility and UV-vis absorption spectroscopy, respectively. The water solubility of 5,7-DMF was increased 361.8-fold by complexation with HPβ-CD and overcame the precipitation problem observed in aqueous buffers, such as during *in vitro* anti-butyrylcholinesterase activity assays. The 1:1 mole ratio of the 5,7-DMF/HPβ-CD complex showed a 2.7-fold higher butyrylcholinesterase inhibitory activity (in terms of the IC_{50} value) compared to the non-complexed compound.

KEY WORDS: 5,7-dimethoxyflavone; butyrylcholinesterase inhibitory activity; hydroxypropyl-β-cyclodextrin; inclusion complex; water solubility.

INTRODUCTION

5,7-Dimethoxyflavone (5,7-DMF) (Fig. 1) is an active and major component in the rhizomes of the medicinal plant *Kaempferia parviflora* Wall. ex Baker in the Zingiberaceae family (1). In Thailand, *K. parviflora* is known as "Thai ginseng" from the belief that the alcoholic decoction from the rhizomes of this plant improves male impotence (aphrodisiac activity). Over the last 5 years, more than 50 publications have reported a variety of pharmaceutical effects of *K. parviflora* tuber extracts, such as anti-inflammatory (2), anti-mutagenic (3), anti-internalization activity of *Helicobacter pylori* (4), aphrodisiac (5) and anti-phosphodiesterase type 5 activities (6). Isolated compounds from *K. parviflora* have also been investigated for their biological activity, and many of them have revealed promising effects. In particular, 5,7-DMF has demonstrated a potential for pharmaceutical therapy. It has been reported to inhibit the inducible nitric oxide synthase (iNOS) expression (7), to exhibit anti-mutagenic activity (3) and to induce endothelium-dependent vasorelaxation through the NO-cGMP pathway and vasodilator prostanoid (8). In addition, 5,7-DMF has butyrylcholinesterase (BChE) inhibitory activity (1) and the ability to inhibit benzo[*a*]pyrene-induced DNA binding and human cytochrome protein expression in the Hep G2 cell line (9) as well as to induce the expression of the breast cancer resistance protein (10). Interestingly, 5,7-DMF, a methylated flavone, was found *in vivo* to have a high oral absorption, bioavailability and tissue distribution (11). Thus, 5,7-DMF is an outstanding candidate chemopreventive/chemotherapeutic agent for many disease treatments. Although 5,7-DMF has a high degree of oral bioavailability, its high hydrophobicity is a serious problem for use as a food supplement or drug development. 5,7-DMF dissolves well in organic solvents, such as chloroform, methanol, ethanol, acetone and DMSO, but these solvents are toxic to normal cells and are not suitable for oral administration. Moreover, 5,7-DMF can precipitate in the bloodstream after injection.

Several reports have attempted to increase the water solubility of drugs or active compounds by complexation with native or derivatized cyclodextrins (CDs) (12–15). CDs are natural cyclic oligosaccharides with a hydrophilic outer surface and a lipophilic central cavity. They can form a non-covalent bond with guest lipophilic molecules and increase their water solubility and biological activity.

Hydroxypropyl-β-cyclodextrin (HPβ-CD), shown in Fig. 1, is a hydroxyalkylated derivative of the native β-CD

Electronic supplementary material The online version of this article (doi:10.1208/s12249-014-0157-0) contains supplementary material, which is available to authorized users.

[1] Petrochemical and Polymer Science Program, Faculty of Science, Chulalongkorn University, Bangkok 10330, Thailand.
[2] Department of Chemistry, Faculty of Science, Chulalongkorn University and Nanotec-CU Center of Excellence on Food and Agriculture, Bangkok 10330, Thailand.
[3] Metallurgy and Materials Science Research Institute, Chulalongkorn University, Bangkok 10330, Thailand.
[4] To whom correspondence should be addressed. (e-mail: p_tiew@hotmail.com)

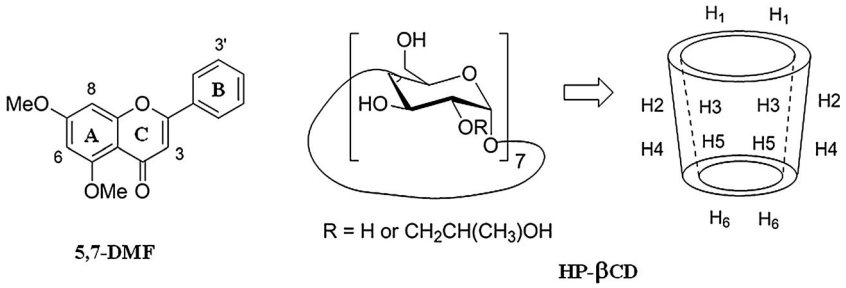

Fig. 1. The chemical structures of 5,7-DMF and HPβ-CD and the positions of the HPβ-CD protons in the structure

but has a higher (>32-fold) water solubility at 600 *vs.* 18.5 mg/mL for HPβ-CD *vs.* β-CD (16). HPβ-CD is commercially available and has already been established to have a high complexing ability and low toxicity. Increases of the water solubility of several bioactive flavonoids, such as taxifolin, genistein, querecetin, kaempferol, myricitin and alpinetin, have been achieved by the formation of inclusion complexes with HPβ-CD (15,17–19). However, those flavonoids contain hydroxyl substituents which are quite different from 5,7-DMF which contains only methoxyl substituents. Although the use of HPβ-CD for the improvement of oral bioavailability of *K. parviflora* crude extract was reported (20), it has not been studied with the pure 5,7-DMF isolated from *K. parviflora* that the complex characterization data are not available. In a preliminary investigation, the complex formation between 5,7-DMF and four different CDs (α-CD, β-CD, γ-CD and HPβ-CD) were prepared, and their water solubility was compared to that of free 5,7-DMF by means of UV-visible (UV-vis) spectroscopy. The results indicated that the inclusion of 5,7-DMF in HPβ-CD showed the highest absorption, assumed to represent the highest water solubility enhancement (data not shown).

Thus, the aim of this work was to improve the water solubility of 5,7-DMF by complexation with HPβ-CD by freeze-drying. The type and stability constant of the complex were determined by phase solubility analysis and Benesi-Hildebrand plot of UV-vis data. Fourier transform infrared spectroscopy (FTIR), X-ray diffraction (XRD), differential scanning calorimetry (DSC), ^{1}H NMR and 2D NMR spectroscopy (rotating frame Overhauser effect spectroscopy, ROESY) and scanning electron microscopy (SEM) were used to characterize the product. Moreover, the *in vitro* BChE inhibitory activity of the 5,7-DMF/HPβ-CD complex was investigated and compared to that for the free 5,7-DMF.

MATERIALS AND METHODS

Materials

5,7-DMF (purity >95%) was isolated from dichloromethane extract of *K. parviflora* rhizomes and purified by silica gel column chromatography as previously described (1). HPβ-CD with an average degree of substitution of 0.6 was purchased from Sigma-Aldrich (Singapore). Butyrylthiocholine iodide (BTCI), 5,5-dithiobis-2-nitrobenzoic acid (DTNB), BChE from horse serum (EC 3.1.1.8) and galanthamine hydrobromide were obtained from Sigma-Aldrich. All other compounds and solvents used in this study were of analytical reagent grade.

Methods

Phase Solubility Studies

Phase solubility studies of 5,7-DMF/HPβ-CD in deionized water were performed as reported (21). An excess amount of 5,7-DMF was added to 25-mL tubes containing 10 mL of an aqueous solution of increasing concentrations of HPβ-CD (0–300 mM). The tubes were sealed, and the mixtures were shaken at 37±0.1°C for 48 h in a thermostatic shaking water bath to reach equilibrium. Then, an aliquot was removed from each tube and filtered through a 0.45-μm PTFE filter, and the 5,7-DMF concentration was determined using an Agilent 8453 UV-Vis spectrophotometer at 264 nm. Each experiment was performed in triplicate. The phase solubility diagram was obtained by plotting the HPβ-CD concentration against the 5,7-DMF concentration. The stability constant (K_s) of 5,7-DMF for HPβ-CD was calculated from the slope and intercept data from the linear regression fitted phase solubility line according to Eq. (1);

$$K_s = \text{(slope)}/[\text{intercept } (1-\text{slope})], \quad (1)$$

where the intercept of the diagram is equal to the solubility of the 5,7-DMF alone.

Stoichiometry Determination: Job's Method

The continuous variation method (22) was performed in order to confirm the stoichiometry of the complex. The sum of the concentration of both components was kept constant ([5,7-DMF] + [HPβ-CD]=1.0×10^{-4} M) whilst the molar fraction of 5,7-DMF (R=[5,7-DMF]/([5,7-DMF] + [HPβ-CD])) varied from 0.0 to 1.0. After stirring for 48 h, the UV absorption at 264 nm was measured for all solutions, and the difference in the absorption between that in the presence (A) and absence of HPβ-CD (A_0), $\Delta A=A-A_0$, was plotted *versus* the molar fraction R. The maximum amount of the complex should occur at the stoichiometric ratio.

Solubility Study

An excess amount of a solid sample (free 5,7-DMF or 5,7-DMF/HPβ-CD complex) was dissolved in 2 mL of water, and it was stirred for 2 h. The solution is then filtered through a 0.45-μm PTFE filter, and the absorbance of the filtrate was recorded at 264 nm.

Determination of the Binding Constant by UV-Vis Spectroscopy

The binding constant (K_b) and stoichiometry of the 5,7-DMF/HPβ-CD inclusion complex were evaluated by Benesi-Hildebrand equation (23). The 5,7-DMF concentration was kept constant (14.4 μM) while the HPβ-CD concentration was varied (0–1.4 mM). The mixtures were left for 24 h before recording the UV absorbance spectra with a UV spectrophotometer (Aligent 8453, C-1103A). The stoichiometry, as either a 1:1 or 1:2 molar ratio, of the complex was determined using Eqs. (2) and (3), respectively:

$$\frac{1}{A-A_0}=\frac{1}{A'-A_0}+\frac{1}{K_b(A-A_0)[\text{HP}\beta\text{-CD}]} \quad (2)$$

$$\frac{1}{A-A_0}=\frac{1}{A'-A_0}+\frac{1}{K_b(A-A_0)[\text{HP}\beta\text{-CD}]^2} \quad (3)$$

A_0, A and A' were the absorbance of 5,7-DMF in the absence of HPβ-CD, in the presence of varied concentrations of HPβ-CD and at the maximum concentration of HPβ-CD. According to Eqs. (2) and (3), the linear plots of either $1/(A-A_0)$ *versus* 1/[HPβ-CD] or 1/[HPβ-CD]^2 that gave the higher correlation coefficient (r^2) determined whether complex was the 1:1 or 1:2 stoichiometry, respectively. The K_b was calculated from the *y*-intercept/slope of the plot.

Preparation of the Inclusion Complex and the Non-complexed Physical Mixture

The inclusion complex of 5,7-DMF/HPβ-CD in a 1:1 molar ratio was prepared by freeze-drying as follows. The solution of 5,7-DMF in ethanol (0.5 mM) was added slowly into the HPβ-CD deionized water solution (0.5 mM) and then magnetically stirred at 40°C for 30 min to remove the ethanol, and then stirring was continued at room temperature for 96 h. Subsequently, the solution was filtered through a 0.45-μm PTFE filter, and the filtrate was freeze-dried for 12 h. The dried inclusion complex was stored in a desiccator until use.

A non-complexed physical mixture of 5,7-DMF and HPβ-CD in a 1:1 mole ratio was prepared by carefully mixing exactly weighed amounts of 5,7-DMF (14 mg or 0.05 mole) and HPβ-CD (69 mg or 0.05 mole) in a ceramic mortar.

Differential Scanning Calorimetry (DSC) Analysis

The DSC curves were obtained using a NETZSCH differential scanning calorimeter model DSC 204 *F1 Phoenix* over the temperature range of 25 to 340°C under nitrogen gas with a heating rate of 10°C/min.

X-ray Powder Diffractometry (XRD) Analysis

XRD patterns were recorded on a Ricoh Dmax 2500 diffractometer, using a Cu Kα radiation (λ=1.5406 Å), in the range of $3° \le 2\theta \ge 50°$ at 25°C (target, Cu; voltage, 40 kV; current, 30 mA).

NMR Spectra

^{1}H NMR spectra of 5,7-DMF (7 mg in 0.5 mL of $CDCl_3$), HPβ-CD (10 mg in 0.5 mL of D_2O) and the 5,7-DMF/HPβ-CD complex (25 mg in 0.5 mL of D_2O) were recorded using a Varian Mercury-400 NMR spectrometer. 2D-ROESY spectra of the inclusion complex (25 mg in 0.5 mL of D_2O) were also measured.

Butyrylcholinesterase (BChE) Inhibitory Activity Assay

The BChE inhibitory activity of the free 5,7-DMF and 5,7-DMF/HPβ-CD complex were determined as previously reported (24). Briefly, 25 μL of 1.5 mM BTCI, 125 μL of 3 mM DTNB, 50 μL of 50 mM Tris-HCl buffer (pH 8) and 25 μL of the test sample were added to each of triplicate wells followed by 25 μL of BChE (1 unit (U)/mL). The absorbance was then read at 415 nm every 5 s for 2 min on a Sunrise microplate reader (P-Intertrade Equipments, Australia) to obtain the velocity of the enzymatic reaction. The inhibitory percentage at each concentration was calculated by subtracting the observed enzyme activity (%) from 100%. At least seven concentrations of each sample were selected in order to obtain the inhibition of the BChE enzyme activity over the range of 20–80%. The concentration of sample required to inhibit 50% of the maximum observed enzymatic activity (IC_{50}) was determined graphically from the log concentration-percent inhibition curves using the GraphPad Prism 5.01 software (GraphPad Software Inc.).

Morphological Analysis

SEM analysis of the surface morphology of each sample was determined on a Philips XL30CP instrument. The samples were placed on a stub and then coated with a thin layer of gold in a vacuum for 30 s.

RESULTS AND DISCUSSION

Phase Solubility, Job's Plot and Solubility Study

The phase solubility diagram of 5,7-DMF within the concentration range of 0–300 mM HPβ-CD is shown in Fig. 2. The solubility of 5,7-DMF increased as a linear function of the HPβ-CD in the concentration range of 0–10 mM (Fig. 2, inset), with a linear regression equation of [5,7-DMF]= 0.023[HPβ-CD]+0.010 (correlation coefficient, R^2 of 0.999). This is consistent with an A_L-type phase solubility (21) and suggests the formation of a 1:1 molar complex. The apparent stability constant (K_s), as calculated according to Eq. (1) (section "Phase Solubility Studies"), was 2.4×10^3 M^{-1}. This value was 2.9-folds higher than that reported for the complex of 5,7-DMF in the crude *K. parviflora* extract (20). Job's method was performed in order to confirm the stoichiometry of the complex. The maximum absorbance variation of 5,7-DMF was observed at a molar fraction of about 0.5 (Supplementary Information (SI); Fig. S1), which indicated that the stoichiometry of the complex 5,7-DMF/HPβ-CD was 1:1, in agreement with the phase solubility study. However, a negative deviation from the linearity was observed when the concentration of HPβ-CD was higher

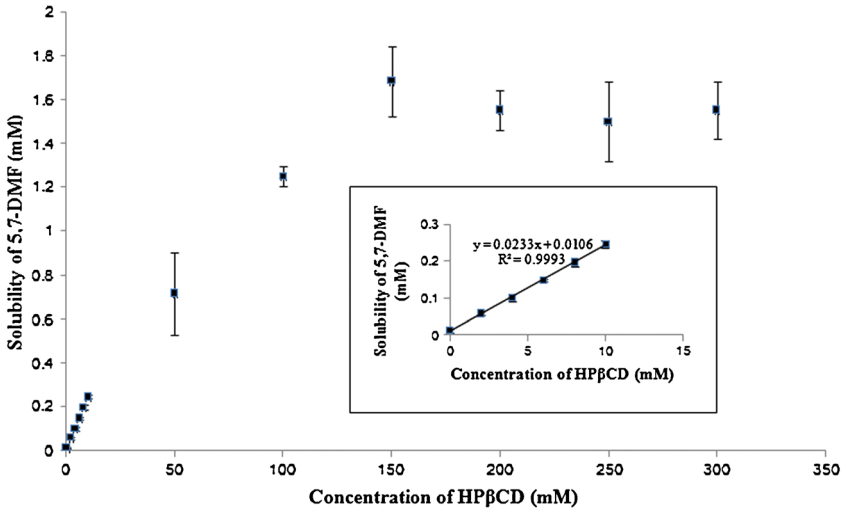

Fig. 2. Phase solubility diagram for the 5,7-DMF/HPβ-CD system in water. Data are shown as the mean ± 1 SD and are derived from three measurements

than 10 mM. The solubility of 5,7-DMF became saturated at ~1.7 mM in the presence of HPβ-CD 150 mM or higher.

The water solubility of free 5,7-DMF and 1:1 mole ratio of 5,7-DMF/HPβ-CD complex was determined by dissolution tests. The solubility of 5,7-DMF in distilled water was significantly increased from 0.00304±0.00095 to 1.10±0.04 mg/mL (361.8-fold enhancement) by complexation with HPβ-CD.

Binding Constant by UV-Vis Spectroscopy

An increased absorbance value of 5,7-DMF with increased HPβ-CD concentrations was observed (Fig. 3), with no detectable shift in the λ_{max} of 5,7-DMF at 264 nm when complexed with HPβ-CD. According to the Benesi-Hildebrand equation, a good linear correlation (r^2=0.9688) was obtained from the plot of $1/(A-A_0)$ as a function of 1/[HPβ-CD] (SI Fig. S2). This supports the formation of an inclusion complex with a 1:1 molar stoichiometry. The binding constant (K_b) of 1.3×10^3 M^{-1} was calculated from the *y*-intercept/slope of the linear plot that was in the same range of that derived from the phase solubility study (2.4×10^3 M^{-1}).

DSC Analysis

The thermal properties of 5,7-DMF, HPβ-CD, the 1:1 molar ratio 5,7-DMF/HPβ-CD complex and the non-complexed 5,7-DMF and HPβ-CD mixture (1:1 molar ratio) were investigated by DSC. The DSC curve of 5,7-DMF showed a sharp endothermic peak at 152.0°C (Fig. 4a), which was attributed to the melting of 5,7-DMF. Two broad endothermic peaks at 96.9°C and above 300°C were detected in the DSC curve of pure HPβ-CD (Fig. 4b), ascribed to the loss of water and HPβ-CD decomposition, respectively, which is in agreement with that reported by de Araújo *et al.* (25). In the DSC

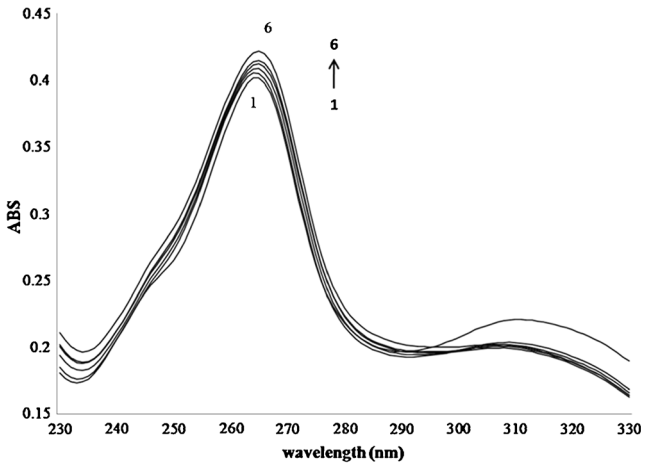

Fig. 3. UV-vis spectra of 5,7-DMF (14.4 μM) in the presence of the following various concentrations of HPβ-CD: (*1*) no HPβ-CD, (*2*) 0.2 mM, (*3*) 0.4 mM, (*4*) 0.6 mM, (*5*) 1.0 mM and (*6*) 1.4 mM

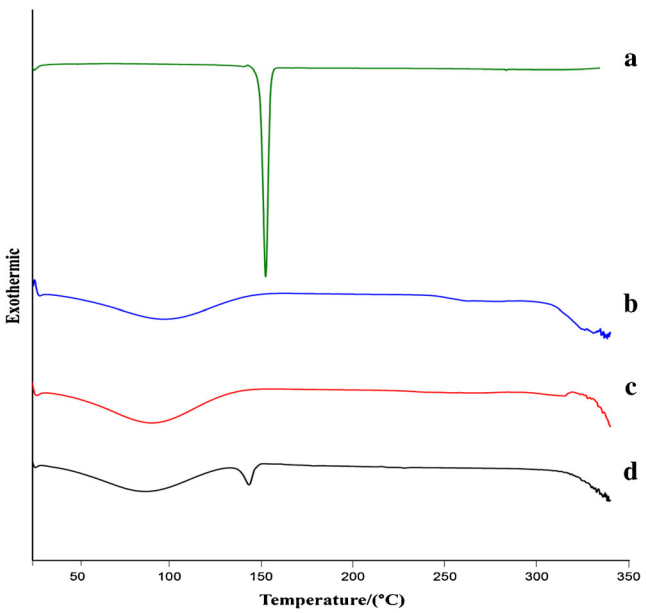

Fig. 4. DSC thermograms of *a* 5,7-DMF, *b* HPβ-CD, *c* lyophilized 1:1 molar 5,7-DMF/HPβ-CD complex and *d* the physical (non-complexed) mixture of 5,7-DMF and HPβ-CD (1:1 molar ratio)

curve of the 5,7-DMF/HPβ-CD complex (Fig. 4c), the endothermic peak of the free 5,7-DMF was absent and that of the HPβ-CD shifted to 89.6°C. This may indicate the interaction of 5,7-DMF in the HPβ-CD cavity, leading to the loss of the crystalline character of 5,7-DMF. In contrast, the DSC curve of the physical mixture (Fig. 4d) showed the simple combination effect of 5,7-DMF and HPβ-CD. Thus, these results support the formation of the 5,7-DMF/HPβ-CD complex.

XRD Analysis

Further evidence for the formation of the 5,7-DMF/HPβ-CD complex was obtained from the powder XRD patterns. Intense and sharp peaks in the diffraction pattern of 5,7-DMF (Fig. 5a) indicated the crystal nature of the compound. In contrast, the XRD pattern of HPβ-CD showed an amorphous structure (Fig. 5b). The diffraction pattern of the lyophilized inclusion complex (Fig. 5c) was clearly distinct from the physical mixture (Fig. 5d). The physical mixture principally displayed the simple combination characteristics of an amorphous cyclodextrin and a crystalline 5,7-DMF, whilst the lyophilized inclusion complex displayed an amorphous structure. The latter pattern was probably due to both the structure of HPβ-CD and the lyophilization process. However, the loss of crystallinity of the complex supported the formation of a new amorphous inclusion complex between 5,7-DMF and HPβ-CD.

^{1}H NMR and ROESY Analyses

The ^{1}H NMR spectroscopy studies of HPβ-CD and the 5,7-DMF/HPβ-CD complexes were performed to evaluate if the inclusion of 5,7-DMF was inside the HPβ-CD cavity. Given that the HPβ-CD H3 and H5 protons inside the hydrophobic cavity were close to the wide and narrow rims of the HPβ-CD cavity, respectively (Fig. 1), then significant chemical shifts of the H3 and H5 protons would result if the guest molecule is located in the HPβ-CD cavity to form an inclusion complex. The ^{1}H NMR data of HPβ-CD with and without 5,7-DMF, and the values of the complexation shifts ($\Delta\delta$), are shown in Table I (see their ^{1}H NMR spectra in SI Fig. S3), where the $\Delta\delta$ of the protons H3 and (especially) H5 (inside the HPβ-CD structure) were indeed larger than the others (H1, H2, H4, H6 and Me) that are located on the outside of the structure. The larger changes are explained by the magnetic anisotropic effect in which the presence of the aromatic benzene moiety of 5,7-DMF caused a shielding effect towards the interior protons of HPβ-CD (26). Thus, these results strongly support the formation of a 5,7-DMF/HPβ-CD inclusion complex.

To gain more information on the inclusion mode, 2D–ROESY analysis was performed to provide correlation through the space proximity of the host and guest protons. The ^{1}H-^{1}H 2D-ROESY spectrum of the 1:1 molar ratio 5,7-DMF/HPβ-CD complex (Fig. 6) showed the correlations of the H3 and H8 protons of 5,7-DMF with the H5 and H6 protons of HPβ-CD, but no correlation was evident between the B-ring protons of 5,7-DMF and the H3 or H5 protons of HPβ-CD. These results indicated that the inclusion of 5,7-DMF involves the A-ring, not the B-ring, which was normally found for other flavones previously reported in the literatures (15,19). Unlike the other flavones reported, the A-ring of 5,7-DMF contains no hydroxyl group which probably furnishes the hydrophobic driving force for its inclusion into the CD cavity.

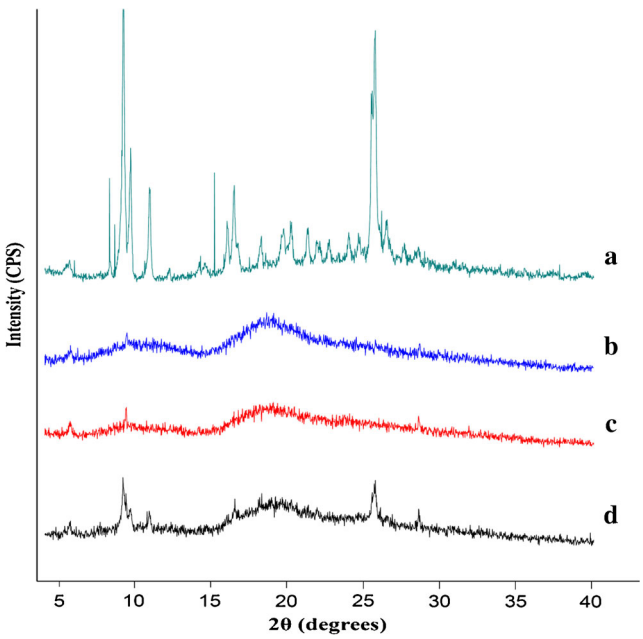

Fig. 5. The XRD patterns of *a* 5,7-DMF, *b* HPβ-CD, *c* lyophilized 1:1 molar 5,7-DMF/HPβ-CD complex and *d* the physical (non-complexed) mixture of 5,7-DMF and HPβ-CD (1:1 molar ratio)

In Vitro BChE Inhibition Activity

BChE is one of the enzymes responsible for the hydrolysis of the neurotransmitter acetylcholine (ACh) in the brain. The significant reduction of ACh level in the elderly people can lead to Alzheimer's disease (AD), and the BChE inhibitors are known to be used for the treatment of this disease (27). 5,7-DMF has previously been shown to exert 85% inhibition of BChE activity at 0.1 mg/mL (1). However, 5,7-DMF has a low solubility under the BChE assay conditions, and its precipitation might lead to erroneous estimates of the actual BChE inhibitory activity. If the water solubility of 5,7-DMF was increased by the inclusion complexation with HPβ-CD, its activity in aqueous buffer may also be increased, if the

Table I. The Proton Chemical Shifts of HPβ-CD and the 1:1 Molar Ratio 5,7-DMF/HPβ-CD Complex, as Determined by NMR Analysis

	δ (ppm)		
	HPβ-CD	5,7-DMF/HPβ-CD complex	$\Delta\delta^a$
H-1	4.885	4.878	−0.007
H-2	3.441	3.436	−0.005
H-3	3.771	3.758	−0.013
H-4	3.399	3.393	−0.006
H-5	3.681	3.644	−0.037
H-6	3.681	3.675	−0.006
Me	0.965	0.956	−0.009

$a = \delta_{(complex)} - \delta_{(HP\beta\text{-}CD)}$

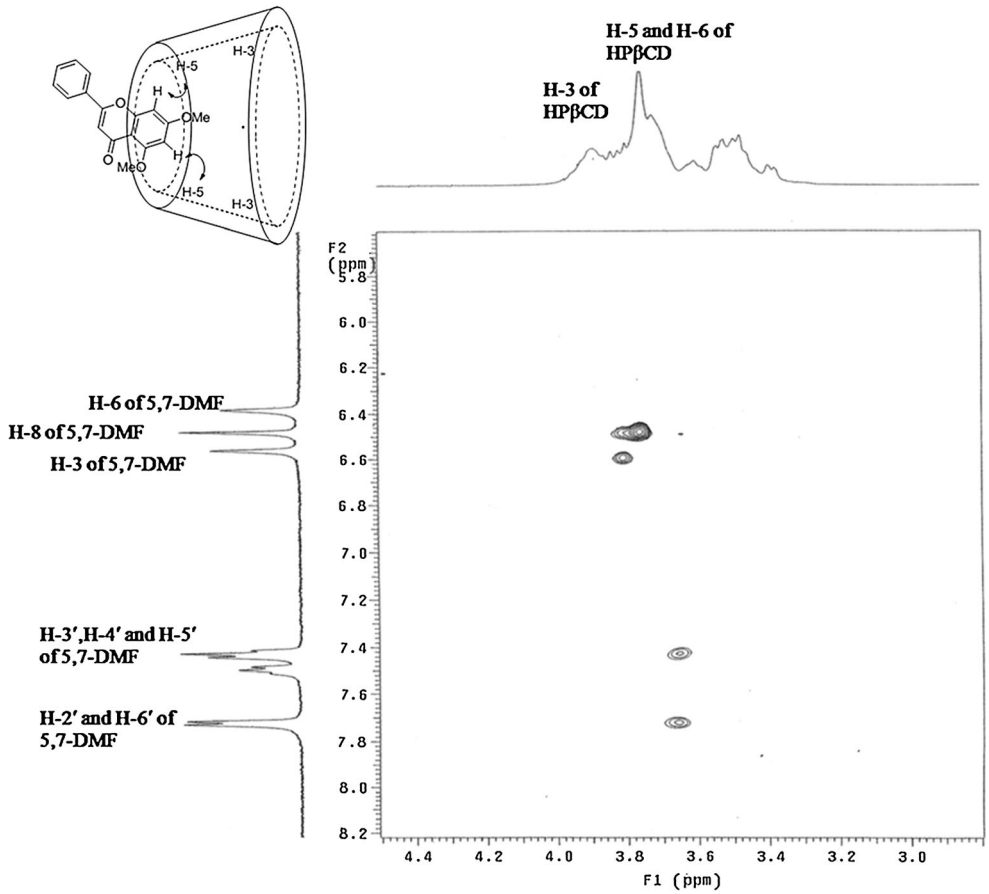

Fig. 6. Portion of the ^{1}H-^{1}H 2D-ROESY spectrum of 5,7-DMF/HPβ-CD complex

complex leads to an increased ability of 5,7-DMF to reach the specific active site of BChE rather than to sequester it away. The inclusion of 5,7-DMF into HPβ-CD improved the water solubility of 5,7-DMF, with no precipitate being seen in distilled water at 10 μg/mL (SI Fig. S4).

The BChE inhibitory activity of 5,7-DMF in the absence and presence of HPβ-CD was measured at final 5,7-DMF concentrations of 5, 10 and 50 μg/mL. Under these concentrations, the free 5,7-DMF precipitated slightly in the assay buffer whereas the 5,7-DMF/HPβ-CD complex remained dissolved as a clear solution. A dose-dependent inhibition of BChE activity was seen for both the free 5,7-DMF and the 5,7-DMF/HPβ-CD complex, but not for HPβ-CD alone (Fig. 7). However, the 5,7-DMF/HPβ-CD complex displayed a 1.66-, 1.22- and 1.22-fold higher inhibitory activity than free 5,7-DMF at 5, 10 and 50 μg/mL, respectively, whilst

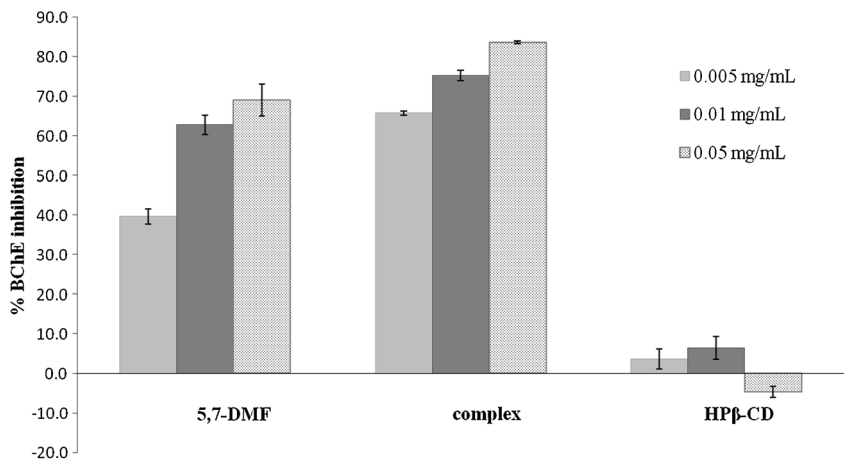

Fig. 7. The BChE inhibition potency of 5,7-DMF, the 5,7-DMF/HPβ-CD complex (1:1 molar ratio) and HPβ-CD. Data are shown as the mean ± 1 SD and are derived from three measurements

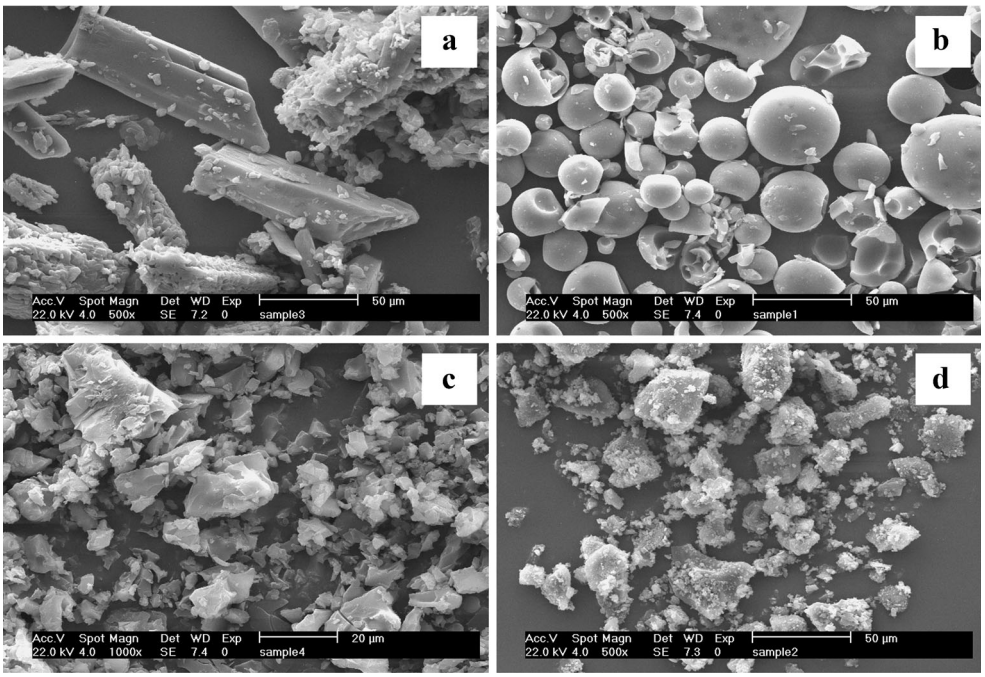

Fig. 8. Scanning electron microphotographs of **a** 5,7-DMF, **b** HPβ-CD, **c** the 5,7-DMF/HPβ-CD complex and **d** the physical mixture of 5,7-DMF and HPβ-CD

the IC_{50} value of the 5,7-DMF/HPβ-CD inclusion complex (23.5±6.4 μM) was 2.7-fold lower than that of free 5,7-DMF (62.4±5.9 μM). The increase of the *in vitro* BChE inhibitory activity of 5,7-DMF in the inclusion complex implies the possibility of this formulation to increase the drug activity for AD treatment.

SEM Analysis

The surface morphological structure of the solid complex and parental components were visualized by SEM. The morphology of pure 5,7-DMF resembled an orthorhombic crystal (Fig. 8a), whilst that of HPβ-CD was shrink-spherical shaped (Fig. 8b). The amorphous plate-like shape of the 5,7-DMF/HPβ-CD inclusion complex did not reveal the original morphology of either parental component (Fig. 8c). In contrast, the physical mixture of 5,7-DMF and HPβ-CD revealed the forms of broken crystals of both parental components (Fig. 8d). These differences in the SEM images further support the formation of an inclusion complex between 5,7-DMF and HPβ-CD.

CONCLUSIONS

The complexation between 5,7-DMF and HPβ-CD was characterized by DSC, XRD and SEM analyses. The phase solubility, Job's plot and Benesi-Hildebrand plot of UV-vis spectroscopic data confirmed the formation of a 1:1 complex. The ^{1}H NMR and ROESY revealed the inclusion of the A ring of 5,7-DMF into the HPβ-CD cavity. The solubility of 5,7-DMF was enhanced by 361.8-fold due to this inclusion complexation, and the BChE inhibitory activity (as IC_{50} value) was increased by 2.7-fold. Thus, the complexation of 5,7-DMF with HPβ-CD is beneficial to food and medical applications of this compound.

ACKNOWLEDGMENTS

This work was financially supported by the Higher Education Research Promotion and National Research University Project of Thailand, the Office of the Higher Education Commission (FW645A), National Research University project of CHE(AM1077I), the Special Task Force for Activating Research (STAR) from the Centenary Academic Development Project, Chulalongkorn University, and the Program of Center of Excellence Network from Nanotechnology Center (NANOTEC), NSTDA, Ministry of Science and Technology, Thailand. The authors are also grateful for English corrections by Robert Butcher of the Publication Counseling Unit, Faculty of Science, Chulalongkorn University.

REFERENCES

1. Sawasdee P, Sabphon C, Sitthiwongwanit D, Kokpol U. Anticholinesterase activity of 7-methoxyflavones isolated from *Kaempferia parviflora*. Phytother Res. 2009;23(12):1792–4.
2. Sae-Wong C, Tansakul P, Tewtrakul S. Anti-inflammatory mechanism of *Kaempferia parviflora* in murine macrophage cells (RAW 264.7) and in experimental animals. J Ethnopharmacol. 2009;124(3):576–80.
3. Azuma T, Kayano SI, Matsumura Y, Konishi Y, Tanaka Y, Kikuzaki H. Antimutagenic and α-glucosidase inhibitory effects of constituents from *Kaempferia parviflora*. Food Chem. 2011;125(2):471–5.
4. Chaichanawongsaroj N, Amonyingcharoen S, Saifah E, Poovorawan Y. The effects of *Kaempferia parviflora* on antiinternalization activity of *Helicobacter pylori* to HEp-2 cells. Afr J Biotechnol. 2010;9(30):4796–801.
5. Wattanathorn J, Pangphukiew P, Muchimapura S, Sripanidkulchai K, Sripanidkulchai B. Aphrodisiac activity of *Kaempferia parviflora*. Am J Agric Biol Sci. 2012;7(2):114–20.
6. Temkitthawon P, Hinds TR, Beavo JA, Viyoch J, Suwanborirux K, Pongamornkul W, *et al. Kaempferia parviflora,* a plant used in traditional medicine to enhance sexual performance contains large amounts of low affinity PDE5 inhibitors. J Ethnopharmacol. 2011;137(3):1437–41.

7. Sae-Wong C, Matsuda H, Tewtrakul S, Tansakul P, Nakamura S, Nomura Y, *et al*. Suppressive effects of methoxyflavonoids isolated from *Kaempferia parviflora* on inducible nitric oxide synthase (iNOS) expression in RAW 264.7 cells. J Ethnopharmacol. 2011;136(3):488–95.
8. Tep-Areenan P, Sawasdee P, Randall M. Possible mechanisms of vasorelaxation for 5,7-dimethoxyflavone from *Kaempferia parviflora* in the rat aorta. Phytother Res. 2010;24(10):1520–5.
9. Wen X, Walle UK, Walle T. 5,7-Dimethoxyflavone downregulates CYP1A1 expression and benzo[*a*]pyrene-induced DNA binding in Hep G2 cells. Carcinogenesis. 2005;26(4):803–9.
10. An G, Wu F, Morris ME. 5,7-Dimethoxyflavone and multiple flavonoids in combination alter the ABCG2-mediated tissue distribution of mitoxantrone in mice. Pharm Res. 2011;28(5):1090–9.
11. Walle T, Ta N, Kawamori T, Wen X, Tsuji PA, Walle UK. Cancer chemopreventive properties of orally bioavailable flavonoids-Methylated versus unmethylated flavones. Biochem Pharmacol. 2007;73(9):1288–96.
12. Yang B, Lin J, Chen Y, Liu Y. Artemether/hydroxypropyl-β-cyclodextrin host-guest system: characterization, phase-solubility and inclusion mode. Bioorg Med Chem. 2009;17(17):6311–7.
13. Dreassi E, Zizzari AT, Mori M, Filippi I, Belfiore A, Naldini A, *et al*. 2-Hydroxypropyl-β-cyclodextrin strongly improves water solubility and anti-proliferative activity of pyrazolo[3,4-*d*]pyrimidines Src-Abl dual inhibitors. Eur J Med Chem. 2010;45(12):5958–64.
14. Pescitelli G, Bilia AR, Bergonzi MC, Vincieri FF, Di Bari L. Cyclodextrins as carriers for kavalactones in aqueous media: spectroscopic characterization of (S)-7,8-dihydrokavain and β-cyclodextrin inclusion complex. J Pharm Biomed Anal. 2010;52(4):479–83.
15. Yang LJ, Chen W, Ma SX, Gao YT, Huang R, Yan SJ, *et al*. Host-guest system of taxifolin and native cyclodextrin or its derivative: preparation, characterization, inclusion mode, and solubilization. Carbohyd Polym. 2011;85(3):629–37.
16. Loftsson T, Duchêne D. Cyclodextrins and their pharmaceutical applications. Int J Pharm. 2007;329(1–2):1–11.
17. Cannavà C, Crupi V, Ficarra P, Guardo M, Majolino D, Mazzaglia A, *et al*. Physico-chemical characterization of an amphiphilic cyclodextrin/genistein complex. J Pharm Biomed Anal. 2010;51(5):1064–8.
18. Mercader-Ros MT, Lucas-Abellán C, Fortea MI, Gabaldón JA, Núñez-Delicado E. Effect of HP-β-cyclodextrins complexation on the antioxidant activity of flavonols. Food Chem. 2010;118(3):769–73.
19. Ma SX, Chen W, Yang XD, Zhang N, Wang SJ, Liu L, *et al*. Alpinetin/hydroxypropyl-β-cyclodextrin host-guest system: preparation, characterization, inclusion mode, solubilization and stability. J Pharm Biomed Anal. 2012;67–68:193–200.
20. Mekjaruskul C, Yang YT, Leed MGD, Sadgrove MP, Jay M, Sripanidkulchai B. Novel formulation strategies for enhancing oral delivery of methoxyflavones in *Kaempferia parviflora* by SMEDDS or complexation with 2-hydroxypropyl-β-cyclodextrin. Int J Pharm. 2013;445(1–2):1–11.
21. Higuchi T, Connors K. Phase solubility techniques. Adv Anal Chem Instrum. 1965;4:117–212.
22. Job P. Job's method of continuous variation. Ann Chim. 1928;9:113–203.
23. Negi JS, Singh S. Spectroscopic investigation on the inclusion complex formation between amisulpride and γ-cyclodextrin. Carbohyd Polym. 2013;92(2):1835–43.
24. Sermboonpaisarn T, Sawasdee P. Potent and selective butyrylcholinesterase inhibitors from *Ficus foveolata*. Fitoterapia. 2012;83(4):780–4.
25. de Araújo MV, Vieira EK, Lázaro GS, de Souza Conegero L, Ferreira OP, Almeida LE, *et al*. Inclusion complexes of pyrimethamine in 2-hydroxypropyl-β-cyclodextrin: characterization, phase solubility and molecular modelling. Bioorg Med Chem. 2007;15(17):5752–9.
26. Veiga FJB, Fernandes CM, Carvalho RA, Geraldes CF. Molecular Modelling and ^{1}H-NMR: Ultimate tools for the investigation of tolbutamide: β-cyclodextrin and tolbutamide: hydroxypropyl-β -cyclodextrin complexes. Chem Pharm Bull. 2001;49(10):1251–6.
27. Greig NH, Lahiri DK, Sambamurti K. Butyrylcholinesterase: an important new target in Alzheimer's disease therapy. Int Psychogeriatr. 2002;14(1):77–91.